

---

# ABOUT LATENT ROLES IN FORECASTING PLAYERS IN TEAM SPORTS

**Luca Scafano, Alessio Sampieri, Giuseppe Re, Matteo Almanza**

**Alessandro Panconesi, Fabio Galasso**

Sapienza University of Rome

{scafano, sampieri}@diag.uniroma1.it

{re, almanza, ale, galasso}@di.uniroma1.it

## ABSTRACT

Forecasting players in sports has grown in popularity due to the potential for a tactical advantage and the applicability of such research to multi-agent interaction systems. Team sports contain a significant social component that influences interactions between teammates and opponents. However, it still needs to be fully exploited. In this work, we hypothesize that each participant has a specific function in each action and that role-based interaction is critical for predicting players' future moves. We create *RolFor*, a novel end-to-end model for Role-based Forecasting. RolFor uses a new module we developed called Ordering Neural Networks (OrderNN) to permute the order of the players such that each player is assigned to a latent role. The latent role is then modeled with a RoleGCN. Thanks to its graph representation, it provides a fully learnable adjacency matrix that captures the relationships between roles and is subsequently used to forecast the players' future trajectories. Extensive experiments on a challenging NBA basketball dataset back up the importance of roles and justify our goal of modeling them using optimizable models. When an oracle provides roles, the proposed RolFor compares favorably to the current state-of-the-art (it ranks first in terms of ADE and second in terms of FDE errors). However, training the end-to-end RolFor incurs the issues of differentiability of permutation methods, which we experimentally review. Finally, this work restates differentiable ranking as a difficult open problem and its great potential in conjunction with graph-based interaction models. Project is available at: <https://www.pinlab.org/aboutlatentroles>

## 1 INTRODUCTION

Recent advances in visual recognition and sequence modeling have enabled novel objectives in athletic performance and sport analytics [Rein & Memmert \(2016\)](#); [Merhej et al. \(2021\)](#); [Morgulev et al. \(2018\)](#). One novel and challenging task is the multi-agent trajectory forecasting (See Fig. 1) of the players as a result of their observed current motion [Li et al. \(2020\)](#); [Hauri et al. \(2021\)](#). The difficulty is due to tactics, tight interaction of team players, the antagonist behavior of opponents, and the role assigned to each player in each action. Traditional trajectory forecasting techniques [Alahi et al. \(2016\)](#); [Giuliani et al. \(2020\)](#); [Huang et al. \(2019\)](#); [Gupta et al. \(2018\)](#); [Mohamed et al. \(2020\)](#) fall short in performance due to their general formulations and lack of sport-specific dynamics. Furthermore, trajectory forecasting methods must deal with the variable numbers of people in each scene (usually absent in games) and do not consider the presence of two opposing teams, the ball, or the finality in the given sport (e.g. scoring). Most recent literature [Li et al. \(2020\)](#); [Hauri et al. \(2021\)](#) has started to address some of these objectives, but, to our knowledge, none has modeled the role of players for specific actions.

We propose RolFor, a novel graph-based encoder-decoder model that performs a robust prediction of the players' future trajectory, utilizing roles to comprehend their interactions. The players' positions and movements on the court often follow pre-defined schemes, so we assume that each player may be assigned a specific role. By proposing a role-based ordering of nodes in the graph, it is possible to establish a player order and learn role-specific relationships.

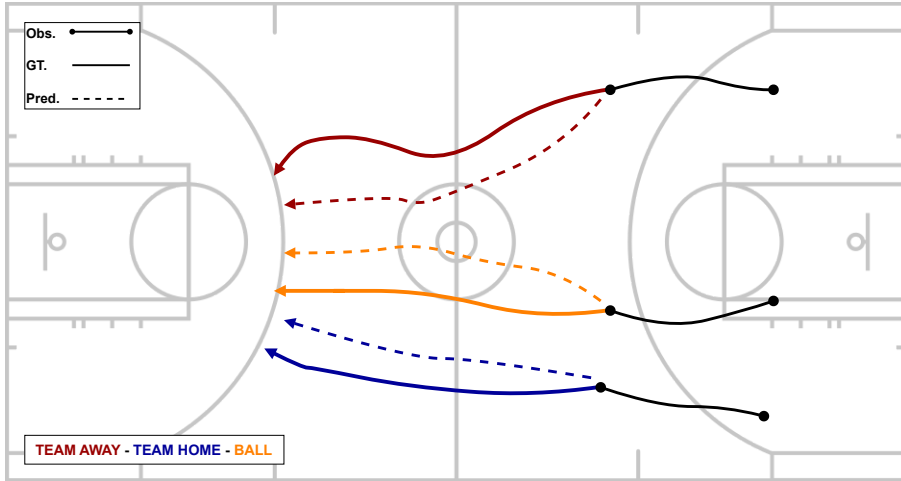


Figure 1: Example of multi-agent trajectory forecasting. We only plot one player for each team and the basketball for readability reasons.

The current best performers in-game forecasting [Li et al. \(2020\)](#); [Mohamed et al. \(2020\)](#) are based on graph convolutional networks (GCN) [Kipf & Welling \(2017\)](#), but they do not consider roles. On the contrary, we model latent roles as nodes in the graph. Our RolFor model is composed of an ordering and a relational module. The former is an Ordering Network, which identifies latent roles and orders players according to them – we use a well-known sorting approximation [Blondel et al. \(2020\)](#) to order the latent projections of the players. In the latter, the game dynamics and trajectories are modeled using RoleGCN, based on [Sofianos et al. \(2021\)](#) where the nodes are the newly assigned roles, and the edges are their relations. The adjacency matrix is learned, and each entry corresponds to learning the role-based player interaction.

We assume roles exist, and many characteristics could dictate them – e.g., marking the opponent, possessing the ball, and identifying the attacking and defending teams. However, we assume no prior knowledge about roles. Our goal is to learn latent roles with an end-to-end algorithm, only considering the future trajectory of all players. To test our intuition about roles, we pre-processed the basketball dataset by assigning roles based on different methods (Table 2) and using those in our RoleGCN. We produce SOTA results, confirming that finding good roles improves model performance. Nevertheless, we found that current differentiable ordering methods face some limitations of backpropagation when inserted in complex models. In summary, our contributions are:

- We experimentally demonstrate that leveraging roles yields SoTA in trajectory forecasting.
- We propose an Order Neural Network module that creates a latent representation of the player’s coordinates and orders them accordingly.
- We build a RoleGCN that learns the relations among roles.
- We empirically demonstrate that the current differentiable ordering approaches have some difficulties with backpropagation – enabling little to no gradients to flow through – when dealing with complex models.

## 2 RELATED WORK

**Trajectory Forecasting** The forecasting of pedestrian movement has been studied to deal with realistic crowd simulation [Pelechano et al. \(2007\)](#) or to improve vehicle collision avoidance [Bhattacharyya et al. \(2018\)](#); it was also used to enhance the accuracy of tracking systems [Choi & Savarese \(2012\)](#); [Pellegrini et al. \(2010\)](#); [Yamaguchi et al. \(2011\)](#) and to study the intentions of individuals or groups of people [Lan et al. \(2012\)](#); [Xie et al. \(2018\)](#). Different models have been proposed to predict such trajectories, like Long Short-Term Memory (LSTM) networks [Hochreiter & Schmidhuber \(1997\)](#) with shared hidden states [Alahi et al. \(2016\)](#), multi-modal Generative Adversarial Networks

---

(GANs) [Gupta et al. \(2018\)](#), or inverse reinforcement learning [Kitani et al. \(2012\)](#). This group forecasting scenario resembles Game Forecasting, where it is necessary to model the movements of two opposing teams.

**Game forecasting** Associations such as National Basketball League or the English Premier League have used sophisticated tracking systems that allow teams to gain insight into each game [Carling et al. \(2008\)](#). Variational Autoencoders (VAEs) were used to model real-world basketball actions, showing that the offensive player trajectories are less predictable than the defense [Felsen et al. \(2018\)](#). LSTM [Seidl et al. \(2010\)](#) were employed to predict near-optimal defensive positions for soccer and basketball, respectively, as for predicting the player’s movements during the game [Hauri et al. \(2021\)](#). Variants of VAEs have also been used [Sun et al. \(2018\)](#) to generate trajectories for NBA players. NBA player trajectory forecasting was also studied in [Zhan et al. \(2018\)](#) and [Zheng et al. \(2017\)](#), proposing a deep generative model based on VAE, LSTM, and RNN [Hauri et al. \(2021\); Hochreiter & Schmidhuber \(1997\); Jain et al. \(2016\)](#) and trained with weak supervision to predict trajectories for an entire team. Nonetheless, we did not encounter work estimating specific latent roles and learning the player interaction on those bases.

**GCN-based forecasting** Adopting a graph structure makes it possible to encode information and quantify shared information between nodes. SoA in pose forecasting learns specific terms for the specific joint-to-joint relation [Sofianos et al. \(2021\); Yan et al. \(2018\)](#). Graphs are also widely used in trajectory forecasting and can be considered fully connected [Li et al. \(2020\)](#), sparse or weighted. These structures distinctly model the interrelationships between nodes, and their combination can be crucial. Also, Graph attention layers (GAT) are widely used in trajectory forecasting [Huang et al. \(2019\); Li et al. \(2021\)](#) to learn the inter-player dependencies. We use the SoA pose forecasting model [Sofianos et al. \(2021\)](#) to model role-based interaction. Pose forecasting is relevant since it considers the fixed node cardinalities and the learned interactions. However, players from various matches and teams do not have a fixed order, which is not an issue with pose forecasting. This encourages us to learn and re-order the players based on hidden roles.

**Differentiable Ranking** Sorting and Ranking are two popular operations in information retrieval that, in our case, can be useful in identifying the role of players. In composition with other functions, sorting induces non-convexity, rendering model parameter optimization difficult. On the other hand, the ranking operation outputs the positions, or ranks, of the input values in the sorted vector. Gradient computation is far more complicated as a piece-wise constant function and could prevent gradient backpropagation. Several recent works [Cuturi et al. \(2019\); Blondel et al. \(2020\)](#) provide an approximation of the above operations for use in a learnable framework.

### 3 METHODOLOGY

This section formally defines the problem and explains our strategy to tackle it, focusing on the role assignment and encoding methods. First, we briefly explain how the Role-based Forecasting model (RoFor) performs latent mapping, role assignment, and trajectory prediction. We also focus on the main components: the Order Neural Network (OrderNN), which handles the ordering task, and the RoleGCN, which facilitates the learning process of relationships between roles in a game.

#### 3.1 PROBLEM FORMALIZATION

We target to predict the future trajectory of all players, given the observed positions at past time frames. We denote the players by 2D vectors  $x_{p,t}$  representing player  $p$  at time  $t$ . The position of all players at time  $t$  are aggregated into a matrix of 2D coordinates  $X_t \in \mathbb{R}^{2 \times p}$ . Motion history of players is denoted by the tensor  $X_{in} = [X_1, X_2, \dots, X_T]$ , which is constructed out of the matrices  $X_t$  for frames  $t = 1, \dots, T$ . The goal is to predict the future  $K$  players positions  $X_{out} = [X_{T+1}, \dots, X_{T+K}]$ .

#### 3.2 ROLE-BASED FORECASTING MODEL (ROLFOR)

RoFor uses two main components, the first one being the OrderNN (Section 3.2.1), which orders players according to their latent roles. We postulate the existence of latent roles that when learned

in an end-to-end architecture yield the best trajectory forecasting performance. From the OrderNN, we will consider  $R$ , the role vector, instead of  $P$ , the position vector. Notice that  $R$  and  $P$  have equal dimensions. The graph is now defined as  $\mathcal{G} = (\mathcal{V}, \mathcal{E})$ , where the nodes indicate the roles of each player and the edges capture the interaction among roles during the game. The graph  $\mathcal{G}$  has  $|\mathcal{V}| = T \times R$  nodes, which represent all  $R$  roles across  $T$  observed time frames. Edges in  $\mathcal{E}$  are represented by a Spatio-Temporal adjacency matrix  $A^{st} \in \mathbb{R}^{RT \times RT}$ , relating the interactions of all roles at all times. Note that  $A^{st}$  is learned, i.e., the model learns how players with different roles interact by learning how latent roles interact over time.

### 3.2.1 ORDER NEURAL NETWORK

The Order Neural Network (Fig. 2) takes in input the initial coordinates  $X_{in}$  and maps them into a latent space. Additionally, it orders the latent vector into optimal roles  $X_{role\_in}$ , thanks to the use of a differentiable ranking method [Blondel et al. \(2020\)](#), which has the same dimensionality of  $X_{in}$ . Note that roles get the corresponding position coordinates over subsequent time frames, so each role is now characterized by a spatio-temporal trajectory. A straightforward example of a role assignment involves sorting players in ascending order based on their Euclidean distance from the ball. This method is also used as a valuable proxy task, which we use for ablation studies (see Section 4 Table 2). However, since RolFor is trained end-to-end, OrderNN is free to learn the ideal ordering that yields the best forecasting performance.

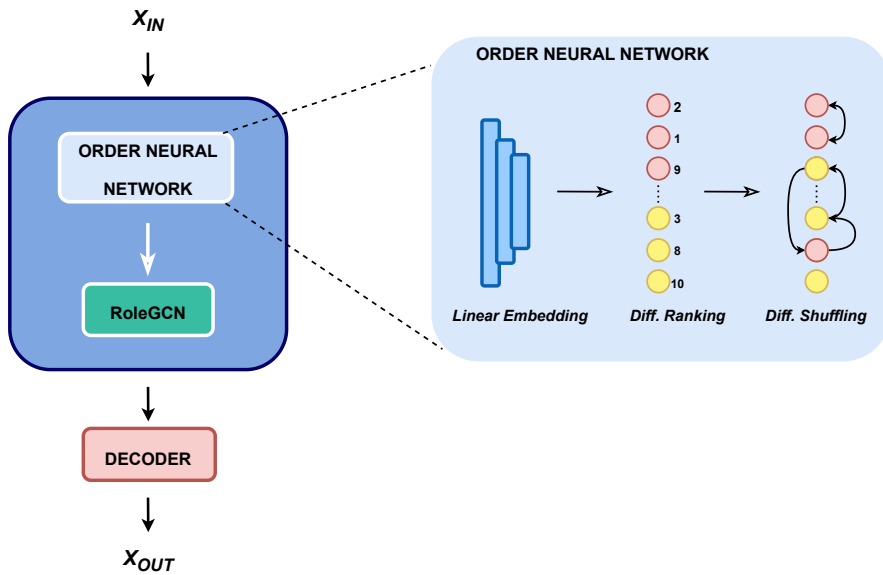


Figure 2: Architecture of RolFor and a zoom into Order Neural Network

**The differentiable ranking method** SoftRank, [Blondel et al. \(2020\)](#) is a recent differentiable implementation of the classic sorting and ranking algorithm, empirically shown to achieve accurate approximation for both tasks. It is designed by constructing differentiable operators as projections onto the permutohedron, i.e., the convex hull of permutations, and using a reduction to isotonic optimization. The key takeaway of the method is to cast sorting and ranking operations as linear programs over the permutohedron. More precisely, it formulates the argsort and ranking operations as optimization problems over the set of permutations  $\Sigma$ . SoftRank also relies on a regularization parameter  $\varepsilon$ , which creates a trade-off between the differentiability of the algorithm and the optimum's accuracy. The greater the regularization factor ( $\varepsilon \rightarrow \infty$ ), the further the approximation from the permutation vertices, and the smoother the loss function gradient. And vice versa, by picking an

---

$\varepsilon \rightarrow 0$ , the algorithm will yield more accurate permutations with a lower degree of differentiability. After learning the ranking, we order the players according to it by employing a differentiable re-shuffling module. The outputs of SoftRank are noted as  $\{s_i\}_{i=1}^n$  where  $n$  is the number of rankings considered. At this point, we use a so-called *base* matrix  $\mathbf{B}$  with the number of rows and columns equal to the number of rankings.  $\mathbf{B}$  will be used to store the real rankings  $\{p_i\}_{i=0}^n$ . We then compute a  $\{\Delta_i\}_{i=1}^n$  matrix, which represents  $\Delta_i = p_i - s_i$  for each position  $\{p_i\}_{i=0}^n$ . The matrix  $\Delta$  is used as the input as a rescaling function. The re-shuffle process is a weighted combination: it yields a real shuffling when the approximated rankings are integer and a differentiable shuffling instead when the ranking is fractional.  $M_i = e^{(\frac{-\Delta}{\text{scale}})^2}$  can be considered an array of weights for each position, with values closer to 1 being the predicted positions of each player. Finally, this will be used to recall the initial coordinates in an ordered manner:

$$P_i = \begin{cases} x'_i = \sum_{j=1}^n M_j \cdot x_j \\ y'_i = \sum_{j=1}^n M_j \cdot y_j \end{cases} \quad (1)$$

### 3.2.2 ROLEGCN

Once the latent roles are inferred, the graph  $\mathcal{G} = (\mathcal{V}, \mathcal{E})$  represents each node  $i \in \mathcal{V}$  as the player's role while the edges  $(i, r) \in \mathcal{E}$  connect all the roles and describe their mutual interaction. RoleGCN (Fig 2) will capture the underlying graph's relationships between different nodes on the court in the same time frame and between one node and itself over different time-frames. GCN [Kipf & Welling \(2017\)](#) is a graph-based operation that works with nodes and edges. For nodes, it aims to learn an embedding containing information about the node itself and its neighborhood for each node in the graph. Thus, the learned adjacency matrices yield a quantitative description of the interplay among roles. The space-time cross-talk is realized by factoring the space-time adjacency matrix (as in [Sofianos et al. \(2021\)](#)) into the product of separate spatial and temporal adjacency matrices  $A^{st} = A^S A^t$ . A separable space-time graph convolutional layer  $l$  is written as follows:

$$H^{(l+1)} = \sigma(A^{s-(l)} A^{t-(l)} \mathcal{H}^{(l)} W^{(l)}) \quad (2)$$

It is similar to a classic GCN convolutional layer, where  $A^{s-(l)} A^{t-(l)}$  is the factorized matrix  $A^{st-(l)}$  of a GCN [Kipf & Welling \(2017\)](#) layer. The critical difference is better efficiency and allows full learnability of the former.

### 3.2.3 DECODER

First, we de-shuffle the permuted roles according to the inverse of  $\mathbf{B}$  to return to the original coordinates' position. The decoding is done with multiple temporal convolutional (TCN) layers [Holden et al. \(2015\)](#) used to predict the following frames. We adopt TCN due to its performance and robustness.

## 4 EXPERIMENTAL EVALUATION

In this section, we introduce the NBA benchmark dataset and metrics, the trajectory forecasting results and investigate why learning E2E roles is challenging.

### 4.1 DATASET

For our experiments, we use NBA SportVU [Felsen et al. \(2018\)](#). It contains players and ball trajectories for 631 games from the 2015-2016 NBA season. Similar to previous work [Sun et al. \(2018\)](#), we focus on just two teams and consider all their games. We obtain a dataset of 95,002, 12-second sequences of players and ball overhead-view trajectories from 1247 games. Each sequence is sampled at 25 Hz, has the same team on offense for the entire duration and ends in a shot, turnover, or foul. As in [Felsen et al. \(2018\)](#), the data is randomly split into train, validation, and test sets with respectively 60,708, 15,244, and 19,050 sequences.

## 4.2 TRAJECTORY FORECASTING METRICS

We use as metrics ADE (Average Displacement Error) and FDE (Final Displacement Error), as usual in literature [Li et al. \(2020\)](#); [Hauri et al. \(2021\)](#); [Alahi et al. \(2016\)](#); [Felsen et al. \(2018\)](#); [Gupta et al. \(2018\)](#). They are used to measure the error of the whole trajectory sequence and the final endpoints for each player. Respectively:

$$ADE = \left\| \hat{T}_c - T_c \right\|_2^2 \quad (3)$$

$$FDE = \left\| \hat{E}_f - E_f \right\|_2^2 \quad (4)$$

Each observation has *five* frames, corresponding to 2.0 seconds in a basketball scenario. The goal is to forecast the successive *ten* frames (4.0 seconds). In Eq. 3,  $\hat{T}_c$  represents the prediction for all future trajectories over the  $c = 1, \dots, 10$  subsequent frames, and  $T_c$  is the ground truth. The same nomenclature is used in Eq. 4, where  $E$  is the matrix for the endpoints and  $c = 1$  since we are only considering the last frame.

## 4.3 TRAJECTORY FORECASTING RESULTS

*So, do roles exist, and does learning the role interaction yields state-of-the-art performance?* We answer this question by considering the most straightforward ordering: Euclidean distance of players from the ball. In Table 1, we report state-of-the-art techniques compared to the RolFor model, with the Euclidean distance ordering of players from the ball. [Li et al. \(2020\)](#) proposes multiple predictions via latent interaction graphs among multiple interactive agents. [Gupta et al. \(2018\)](#), similarly, is also a multi-modal model incorporating the social aspects of the players as well. [Huang et al. \(2019\)](#) is based on a sequence-to-sequence architecture to predict the future trajectories of players. Lastly, [Mohamed et al. \(2020\)](#) substitutes the need for aggregation by modeling the interactions as a graph. Similar to [Yan et al. \(2018\)](#), it needs a pre-defined graph, allowing the learning procedure only on the given edges. RolFor in Table 1 yields the SoA forecasting performance in terms of ADE, 5.55 meters, second best in terms of FDE, 9.99 meters. It sorts players according to their Euclidean distance from the ball, arranging them into a sequence of attackers (players detaining the ball in the considered action), alternating with defenders (not detaining the ball). Each attacker is followed by its marker, which RolFor considers the closest to it in terms of Euclidean distance. As for all other reported SoA algorithms, RolFor considers that the teams are known. Finally, "Oracular Permutation" means that RolFor uses distances at the last future step, i.e., step 10 in the future. In contrast, any other reported algorithm uses only the observed five frames. We will investigate this more thoroughly in the next section. A neural network can learn the Euclidean distance, and softRank [Blondel et al. \(2020\)](#) should be able to sort the players according to it. Replacing the hand-defined distance computation with a Neural Network should be as effective. We expect that a model with a sorting unit that learns sorting E2E in relation to the final forecasting goal should be capable of doing better than this, assuming all modules are effectively differentiable.

Model	ADE	FDE
EvolveGraph <a href="#">Li et al. (2020)</a>	5.73	<b>8.65</b>
Social-STGCNN <a href="#">Mohamed et al. (2020)</a>	6.42	10.04
STGAT <a href="#">Huang et al. (2019)</a>	7.06	12.54
SGAN <a href="#">Gupta et al. (2018)</a>	5.88	10.36
<b>RolFor</b> + Oracular Permutation	<b>5.55</b>	9.99

Table 1: Comparison of our model with SoTA models

### 4.3.1 FURTHER EXPERIMENTS ON EUCLIDEAN ORDERING

We delve deeper into the results of RolFor in Table 1 and analyze the importance of each hand-defined Euclidean distance term in Table 2.

*No ordering Vs. Simple ordering.* The first forecasting result in the table neglects the player ordering and learns interaction terms between players, arranged in random order. It yields 6.34/11.5 ADE/FDE meters errors. Simple ordering stands for arranging all players in a list, according to their distance from the ball, at the last (5th) observed frame. This uncomplicated ordering is only negligibly better than no order. A GCN model may deal with players in random order well and only benefits from ordering if it is informative.

*Distance from the ball and marking.* Results in the third row of the Table 2 add marking to the ball distance ordering. Each player in the attacker team is matched with one from the defender team according to Euclidean distance. Performance improves in ADE, from 6.31 to 6.16 meters, and slightly degrades in terms of FDE, from 11.1 to 11.28. Overall All distances are computed at the last observed frame. Furthermore, all distances are plain Euclidean distances, which a simple Neural Network may replicate or improve with E2E learning.

*Distance from the ball and marking at future frames.* The last row of Table 2 considers the furthest future frame position for all distance computations. It should be noted that the model makes no assumptions about future locations. Future information is simply utilized to place players in order. This motivates us to replace the hand-defined ordering with an E2E-trained module, which we will do in the following section.

Ball Dist.	Obs.	Future	Mark	ADE	FDE
-	-	-	-	6.34	11.5
✓	-	-	-	6.31	11.1
✓	✓	-	✓	6.16	11.28
✓	-	✓	✓	5.55	9.99

Table 2: Results for different types of ordering

#### 4.4 END-TO-END MODEL WITH LATENT ROLES

In this section, we leverage the full RolFor model, E2E trained. Here the first module, OrderNN, sorts players into their roles in the action, then the RoleGCN module reasons on their role-based interaction. Sorting into roles has benefited forecasting in Sec. 4.3.1. Here we assume that roles are latent variables, which the OrderNN estimates, E2E, based on the best forecasting performance. Table 3a compares the hand-defined baseline (ball and marking distance on the last observed frame, scoring 6.16/11.28) against E2E model variants. *E2E* is learning to order, encode the role-role interaction, and forecast based on the encoder. This model is performing poorly at 12.12/15.02 ADE/FDE. Is this because the OrderNN is incapable of ordering, or is it because the OrderNN is not fully differentiable? Moreover, the *EuclDistEst* variant attempts to answer part of this question. Here we used a pre-trained Neural Network module to approximate the Euclidean distance based on the player’s performance. We then use the pre-trained module to sort players according to the ball. If the Euclidean distance estimator model were perfect, performance would be 6.31/11.1 (ADE/FDE), cf. Table 2. *EuclDistEst* yields, however, 7.50/12.58. We attribute this mismatch to the residual errors in the Euclidean distance estimation, which, as it seems, matters. More surprisingly, *E2E-finetune* starts from the *EuclDistEst* variant, and it fine-tunes it, E2E. The error increases to 12.08/14.97, so the model neglects the initialization and reverts to the *E2E* performance. We attribute the discrepancy between *EuclDistEst* and *E2E* to the challenges in the SoftRank differentiability, as we further analyze in the next section.

Configuration	ADE	FDE	Model	ADE	FDE
			Oracular Ordering	5.55	9.99
<i>E2E</i>	12.12	15.02	Light Swap	6.55	12.10
<i>E2E-finetune</i>	12.08	14.97	Light Insert	6.55	12.10
<i>EuclDistEst</i>	7.50	12.58	Light Swap + Light Insert	6.59	12.08
<i>Best non-or. dist.</i>	6.16	11.28	Heavy Swap + Heavy Insert	6.71	12.25

(a) Different training configurations for RolFor

(b) Analysis of simulated errors in ordering

Table 3: Analysis on ADE and FDE for different approaches

---

#### 4.4.1 ANALYSIS OF THE ORDER NEURAL NETWORK

Here we focus on confirming our claims on the issues of the differentiability of Sofrank. We set to order the players according to their ascending distance from the ball, at a specific frame, given their 2D coordinates. It allows us to test the first RolFor module, OrderNN, in isolation, cf.4. In Table 4, we compare *OrderNN E2E* against *OrderNN EuclDistEst*. The first E2E trains the order of players and re-shuffles them. The second supervises the network by tasking it to learn the Euclidean distance between the players and the ball and then sort the distances according to SoftRank. We measure the ordering accuracy  $p_{\text{ord}}$  as the percentage of players the models place in the correct order. In other words, we reproduce the top-k classification experiment as [Cuturi et al. \(2019\)](#). The authors propose a loss for top-k classification between a ground truth class  $ord \in [n]$  and a vector of soft ranks  $\hat{ord} \in \mathbb{R}^n$ , which is higher if the predicted soft ranks correctly place  $y$  in the top-k elements.

Model	top-k	Accuracy
OrderNN <i>E2E</i>	10	1,00%
OrderNN <i>EuclDistEst</i>	10	71,00%
OrderNN <i>EuclDistEst</i>	5	77,00%
OrderNN <i>EuclDistEst</i>	3	82,00%
OrderNN <i>EuclDistEst</i>	1	92,00%

Table 4: OrderNN *E2E* against OrderNN *EuclDistEst* top-k accuracy

Observe from Table 4 that learning Euclidean distances from 2D positions is an easier task for a deep neural network since SoftRank yields 71% at the *top-10* ordering accuracy  $p_{\text{ord}}$ . It is also interesting to notice that when changing the *top-k* ordering accuracy into 5, 3, 1, we get similar results to [Blondel et al. \(2020\)](#). By contrast, learning the ordering E2E from the 2D coordinates yields surprisingly low performance. The table shows that *OrderNN E2E* achieves a *top-10* ordering accuracy of only 1%.

#### 4.5 ROBUSTNESS OF ROLFOR TO ORDERING ERRORS

How much does misordering impact forecasting? We measure ADE and FDE forecasting errors when randomly altering the order provided by our best performing oracle RolFor (5.55/9.99 ADE/FDE, Table 2). In more detail, we consider the swap of two players *Light Swap*, which can occur if the distance between them is relatively small. A more significant error can also occur, e.g., one role is not identified correctly and a player is inserted at the wrong position, making the whole order slip. We name this *Light Insert*. In Table 3b, we consider the two potential sources of errors by randomly simulating one or both. The results are coherent with what we said previously Table 4, where the RolFor *EuclDistEst* has a *top-10* ordering accuracy of 71% yielding 7.50/12.58. At the same time, a Light Swap/Insert gives 6.55/12.10 in ADE/FDE and 80% *top-10* ordering accuracy. This last Table 3b highlights the importance of roles and their impact on the final trajectory accuracy.

### 5 CONCLUSIONS

Our goal was to show that roles and social relations in sports are quantifiable and can be effectively used to improve the current SoA models in game forecasting. We demonstrate that roles exist by testing different permutations over players. Then, we encode the player’s coordinates into a latent space and use the encoding to find an optimal latent role ordering. The model employed to perform trajectory forecasting is called RolFor (Role Forecasting) and considers the input nodes of a graph indicating roles in a game. This single-graph framework favors the relation between roles and time, allowing better learning of the fully-trainable adjacency matrices for role-role and time-time interactions. The adoption of CNNs and the graph structure of the input allows the requirement of parameters to be only a fraction of the ones used in Transformers, GANs, and VAEs. Our observations emphasize the significant opportunity for future work to develop fully differentiable ordering modules to enable learning latent role-based interactions in graph-based models, also applicable to social networks and multi-agent systems.

---

**Acknowledgements** This work was partially supported by the MUR PNRR project FAIR (PE00000013)

## REFERENCES

Alexandre Alahi, Kratarth Goel, Vignesh Ramanathan, Alexandre Robicquet, Li Fei-Fei, and Silvio Savarese. Social lstm: Human trajectory prediction in crowded spaces. In *2016 IEEE Conference on Computer Vision and Pattern Recognition (CVPR)*, pp. 961–971, 2016. doi: 10.1109/CVPR.2016.110.

Apratim Bhattacharyya, Mario Fritz, and Bernt Schiele. Long-term on-board prediction of people in traffic scenes under uncertainty. In *Proceedings of the IEEE Conference on Computer Vision and Pattern Recognition*, pp. 4194–4202, 2018.

Mathieu Blondel, Olivier Teboul, Quentin Berthet, and Josip Djolonga. Fast differentiable sorting and ranking. In *International Conference on Leadership and Management (ICLM)*, 2020. doi: <https://doi.org/10.48550/arXiv.2002.08871>.

Christopher Carling, Jonathan Bloomfield, Lee Nelsen, and Thomas Reilly. The role of motion analysis in elite soccer. *Sports medicine*, 38(10):839–862, 2008.

W. Choi and S. Savarese. A unified framework for multi-target tracking and collective activity recognition. pp. 215–230, 2012.

Marco Cuturi, Olivier Teboul, and Jean-Philippe Vert. Differentiable ranking and sorting using optimal transport. In H. Wallach, H. Larochelle, A. Beygelzimer, F. d'Alché-Buc, E. Fox, and R. Garnett (eds.), *Advances in Neural Information Processing Systems*, volume 32. Curran Associates, Inc., 2019.

Panna Felsen, Patrick Lucey, and Sujoy Ganguly. Where will they go? predicting finegrained adversarial multi-agent motion using conditional variational autoencoders. In *Proceedings of the European Conference on Computer Vision (ECCV)*, pp. 732–747, 2018.

Francesco Giuliani, Irtiza Hasan, Marco Cristani, and Fabio. Galasso. Transformer networks for trajectory forecasting. In *In The International Conference on Pattern Recognition (ICPR)*, 2020. doi: <https://doi.org/10.48550/arXiv.2003.08111>.

Agrim Gupta, Justin Johnson, Li Fei-Fei, Silvio Savarese, and Alexandre Alahi. Social gan: Socially acceptable trajectories with generative adversarial networks. In *2018 IEEE/CVF Conference on Computer Vision and Pattern Recognition*, pp. 2255–2264, 2018. doi: 10.1109/CVPR.2018.00240.

Sandro Hauri, Nemanja Djuric, Vladan Radosavljevic, and Slobodan Vucetic. Multi-modal trajectory prediction of nba players. In *Winter Conf. on Applications of Computer Vision (WACV)*, 2021. doi: <https://doi.org/10.48550/arXiv.2008.07870>.

Sepp Hochreiter and Jürgen Schmidhuber. Long short-term memory. In *Neural Computation*, pp. 1735—1780, 1997. doi: 10.1162/neco.1997.9.8.1735.

Daniel Holden, Jun Saito, Taku Komura, and Thomas Joyce. Learning motion manifolds with convolutional autoencoders. In *SIGGRAPH Asia*, 2015. doi: <https://doi.org/10.1145/2820903.2820918>.

Yingfan Huang, Huikun Bi, Zhaoxin Li, Tianlu Mao, and Zhaoqi Wang. Stgat: Modeling spatial-temporal interactions for human trajectory prediction. In *ICCV*, 2019.

Ashesh Jain, Amir Zamir, Silvio Savarese, and Ashutosh Saxena. Structural-rnn: Deep learning on spatio-temporal graph. In *The IEEE Computer Vision and Pattern Recognition (CVPR)*, 2016. doi: <https://doi.org/10.48550/arXiv.1511.05298>.

T.N. Kipf and M Welling. Semi-supervised classification with graph convolutional networks. In *ICLR*, 2017.

---

K. M. Kitani, B. D. Ziebart, J. A. Bagnell, and M. Hebert. Activity forecasting. In *In European Conference on Computer Vision ECCV*, pp. 201–214, 2012.

Tian Lan, Yang Wang, Weilong Yang, Stephen N. Robinovitch, and Greg Mori. Discriminative latent models for recognizing contextual group activities. volume 34(8), pp. 1549–1562, 2012.

Jiachen Li, Fan Yang, Masayoshi Tomizuka, and Chiho Choi. Evolvegraph: Multi-agent trajectory prediction with dynamic relational reasoning. 10 2020. doi: <https://doi.org/10.48550/arXiv.2003.13924>.

Longyuan Li, Jian Yao, Li Wenliang, Tong He, Tianjun Xiao, Junchi Yan, David Wipf, and Zheng Zhang. Grin: Generative relation and intention network for multi-agent trajectory prediction. *Advances in Neural Information Processing Systems*, 34, 2021.

Charbel Merhej, Ryan J Beal, Tim Matthews, and Sarvapali Ramchurn. What happened next? using deep learning to value defensive actions in football event-data. In *Proceedings of the 27th ACM SIGKDD Conference on Knowledge Discovery & Data Mining*, pp. 3394–3403, 2021.

Abduallah Mohamed, Kun Qian, Mohamed Elhoseiny, and Christian Claudel. Social-stgcn: A social spatio-temporal graph convolutional neural network for human trajectory prediction. In *CVPR*, 2020.

Elia Morgulev, Ofer H Azar, and Ronnie Lidor. Sports analytics and the big-data era. *International Journal of Data Science and Analytics*, 5(4):213–222, 2018.

Nuria Pelechano, Jan M. Allbeck, and Norman I. Badler. Controlling individual agents in high-density crowd simulation. In *SCA '07*, 2007.

Stefano Pellegrini, Andreas Ess, and Luc Van Gool. Improving data association by joint modeling of pedestrian trajectories and groupings. In *ECCV*, 2010.

Robert Rein and Daniel Memmert. Big data and tactical analysis in elite soccer: future challenges and opportunities for sports science. *SpringerPlus*, 5(1):1–13, 2016.

T. Seidl, A. Cherukumudi, A. T. Hartnett, P. Carr, and P. Lucey. Bhostgusters : Realtime interactive play sketching with synthesized nba defenses. In *MIT Sloan Sports Analytics COnference*, 2010.

Theodoros Sofianos, Alessio Sampieri, Luca Franco, and Fabio Galasso. Space-time-separable graph convolutional network for pose forecasting. In *International Conference on Computer Vision (ICCV)*, 2021. doi: <https://doi.org/10.48550/arXiv.2110.04573>.

Chen Sun, Per Karlsson, Jiajun Wu, Joshua Tenenbaum, and Kevin Murphy. Stochastic prediction of multi-agent interactions from partial observations. 09 2018. doi: <https://doi.org/10.48550/arXiv.1902.09641>.

Dan Xie, Tianmin Shu, Sinisa Todorovic, and Song-Chun Zhu. Learning and inferring “dark matter” and predicting human intents and trajectories in videos. volume 40(7), pp. 1639–1652, 2018. doi: 10.1109/TPAMI.2017.2728788.

Kota Yamaguchi, Alexander C. Berg, Luis E. Ortiz, and Tamara L. Berg. Who are you with and where are you going? In *CVPR 2011*, pp. 1345–1352, 2011. doi: 10.1109/CVPR.2011.5995468.

Sijie Yan, Yuanjun Xiong, and Dahua Lin. Spatial temporal graph convolutional networks for skeleton-based action recognition. In *AAAI*, 2018.

Eric Zhan, Stephan Zheng, Yisong Yue, Long Sha, and Patrick Lucey. Generating multi-agent trajectories using programmatic weak supervision. 03 2018. doi: <https://doi.org/10.48550/arXiv.1803.07612>.

Stephan Zheng, Yisong Yue, and Patrick Lucey. Generating long-term trajectories using deep hierarchical networks. 06 2017. doi: <https://doi.org/10.48550/arXiv.1706.07138>.

---

# FORMATTING INSTRUCTIONS FOR ICLR 2023 CONFERENCE SUBMISSIONS

## Anonymous authors

### ABSTRACT

The abstract paragraph should be indented 1/2 inch (3 picas) on both left and right-hand margins. Use 10 point type, with a vertical spacing of 11 points. The word ABSTRACT must be centered, in small caps, and in point size 12. Two line spaces precede the abstract. The abstract must be limited to one paragraph.

## 1 SUBMISSION OF CONFERENCE PAPERS TO ICLR 2023

ICLR requires electronic submissions, processed by <https://openreview.net/>. See ICLR’s website for more instructions.

If your paper is ultimately accepted, the statement `\iclrfinalcopy` should be inserted to adjust the format to the camera ready requirements.

The format for the submissions is a variant of the NeurIPS format. Please read carefully the instructions below, and follow them faithfully.

### 1.1 STYLE

Papers to be submitted to ICLR 2023 must be prepared according to the instructions presented here.

Authors are required to use the ICLR  $\text{\LaTeX}$  style files obtainable at the ICLR website. Please make sure you use the current files and not previous versions. Tweaking the style files may be grounds for rejection.

### 1.2 RETRIEVAL OF STYLE FILES

The style files for ICLR and other conference information are available online at:

<http://www.iclr.cc/>

The file `iclr2023_conference.pdf` contains these instructions and illustrates the various formatting requirements your ICLR paper must satisfy. Submissions must be made using  $\text{\LaTeX}$  and the style files `iclr2023_conference.sty` and `iclr2023_conference.bst` (to be used with  $\text{\LaTeX}2e$ ). The file `iclr2023_conference.tex` may be used as a “shell” for writing your paper. All you have to do is replace the author, title, abstract, and text of the paper with your own.

The formatting instructions contained in these style files are summarized in sections 2, 3, and 4 below.

## 2 GENERAL FORMATTING INSTRUCTIONS

The text must be confined within a rectangle 5.5 inches (33 picas) wide and 9 inches (54 picas) long. The left margin is 1.5 inch (9 picas). Use 10 point type with a vertical spacing of 11 points. Times New Roman is the preferred typeface throughout. Paragraphs are separated by 1/2 line space, with no indentation.

Paper title is 17 point, in small caps and left-aligned. All pages should start at 1 inch (6 picas) from the top of the page.

---

Authors' names are set in boldface, and each name is placed above its corresponding address. The lead author's name is to be listed first, and the co-authors' names are set to follow. Authors sharing the same address can be on the same line.

Please pay special attention to the instructions in section 4 regarding figures, tables, acknowledgments, and references.

There will be a strict upper limit of 9 pages for the main text of the initial submission, with unlimited additional pages for citations.

### 3 HEADINGS: FIRST LEVEL

First level headings are in small caps, flush left and in point size 12. One line space before the first level heading and 1/2 line space after the first level heading.

#### 3.1 HEADINGS: SECOND LEVEL

Second level headings are in small caps, flush left and in point size 10. One line space before the second level heading and 1/2 line space after the second level heading.

##### 3.1.1 HEADINGS: THIRD LEVEL

Third level headings are in small caps, flush left and in point size 10. One line space before the third level heading and 1/2 line space after the third level heading.

## 4 CITATIONS, FIGURES, TABLES, REFERENCES

These instructions apply to everyone, regardless of the formatter being used.

### 4.1 CITATIONS WITHIN THE TEXT

Citations within the text should be based on the `natbib` package and include the authors' last names and year (with the "et al." construct for more than two authors). When the authors or the publication are included in the sentence, the citation should not be in parenthesis using `\citet{}` (as in "See ? for more information."). Otherwise, the citation should be in parenthesis using `\citep{}` (as in "Deep learning shows promise to make progress towards AI (?).").

The corresponding references are to be listed in alphabetical order of authors, in the REFERENCES section. As to the format of the references themselves, any style is acceptable as long as it is used consistently.

### 4.2 FOOTNOTES

Indicate footnotes with a number<sup>1</sup> in the text. Place the footnotes at the bottom of the page on which they appear. Precede the footnote with a horizontal rule of 2 inches (12 picas).<sup>2</sup>

### 4.3 FIGURES

All artwork must be neat, clean, and legible. Lines should be dark enough for purposes of reproduction; art work should not be hand-drawn. The figure number and caption always appear after the figure. Place one line space before the figure caption, and one line space after the figure. The figure caption is lower case (except for first word and proper nouns); figures are numbered consecutively.

Make sure the figure caption does not get separated from the figure. Leave sufficient space to avoid splitting the figure and figure caption.

---

<sup>1</sup>Sample of the first footnote

<sup>2</sup>Sample of the second footnote

---

Table 1: Sample table title

PART	DESCRIPTION
Dendrite	Input terminal
Axon	Output terminal
Soma	Cell body (contains cell nucleus)

You may use color figures. However, it is best for the figure captions and the paper body to make sense if the paper is printed either in black/white or in color.

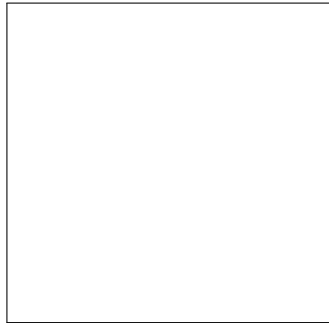


Figure 1: Sample figure caption.

#### 4.4 TABLES

All tables must be centered, neat, clean and legible. Do not use hand-drawn tables. The table number and title always appear before the table. See Table 1.

Place one line space before the table title, one line space after the table title, and one line space after the table. The table title must be lower case (except for first word and proper nouns); tables are numbered consecutively.

#### 5 DEFAULT NOTATION

In an attempt to encourage standardized notation, we have included the notation file from the textbook, *Deep Learning* ? available at [https://github.com/goodfeli/dlbook\\_notation/](https://github.com/goodfeli/dlbook_notation/). Use of this style is not required and can be disabled by commenting out `math_commands.tex`.

##### Numbers and Arrays

---

$a$	A scalar (integer or real)
$\mathbf{a}$	A vector
$\mathbf{A}$	A matrix
$\mathbf{A}$	A tensor
$\mathbf{I}_n$	Identity matrix with $n$ rows and $n$ columns
$\mathbf{I}$	Identity matrix with dimensionality implied by context
$\mathbf{e}^{(i)}$	Standard basis vector $[0, \dots, 0, 1, 0, \dots, 0]$ with a 1 at position $i$
$\text{diag}(\mathbf{a})$	A square, diagonal matrix with diagonal entries given by $\mathbf{a}$
$\mathbf{a}$	A scalar random variable
$\mathbf{a}$	A vector-valued random variable
$\mathbf{A}$	A matrix-valued random variable

### Sets and Graphs

$\mathbb{A}$	A set
$\mathbb{R}$	The set of real numbers
$\{0, 1\}$	The set containing 0 and 1
$\{0, 1, \dots, n\}$	The set of all integers between 0 and $n$
$[a, b]$	The real interval including $a$ and $b$
$(a, b]$	The real interval excluding $a$ but including $b$
$\mathbb{A} \setminus \mathbb{B}$	Set subtraction, i.e., the set containing the elements of $\mathbb{A}$ that are not in $\mathbb{B}$
$\mathcal{G}$	A graph
$\text{Pa}_{\mathcal{G}}(\mathbf{x}_i)$	The parents of $\mathbf{x}_i$ in $\mathcal{G}$

### Indexing

$a_i$	Element $i$ of vector $\mathbf{a}$ , with indexing starting at 1
$a_{-i}$	All elements of vector $\mathbf{a}$ except for element $i$
$A_{i,j}$	Element $i, j$ of matrix $\mathbf{A}$
$\mathbf{A}_{i,:}$	Row $i$ of matrix $\mathbf{A}$
$\mathbf{A}_{:,i}$	Column $i$ of matrix $\mathbf{A}$
$\mathbf{A}_{i,j,k}$	Element $(i, j, k)$ of a 3-D tensor $\mathbf{A}$
$\mathbf{A}_{:, :, i}$	2-D slice of a 3-D tensor
$\mathbf{a}_i$	Element $i$ of the random vector $\mathbf{a}$

### Calculus

---

$\frac{dy}{dx}$	Derivative of $y$ with respect to $x$
$\frac{\partial y}{\partial x}$	Partial derivative of $y$ with respect to $x$
$\nabla_{\mathbf{x}} y$	Gradient of $y$ with respect to $\mathbf{x}$
$\nabla_{\mathbf{X}} y$	Matrix derivatives of $y$ with respect to $\mathbf{X}$
$\nabla_{\mathbf{X}} y$	Tensor containing derivatives of $y$ with respect to $\mathbf{X}$
$\frac{\partial f}{\partial \mathbf{x}}$	Jacobian matrix $\mathbf{J} \in \mathbb{R}^{m \times n}$ of $f : \mathbb{R}^n \rightarrow \mathbb{R}^m$
$\nabla_{\mathbf{x}}^2 f(\mathbf{x})$ or $\mathbf{H}(f)(\mathbf{x})$	The Hessian matrix of $f$ at input point $\mathbf{x}$
$\int f(\mathbf{x}) d\mathbf{x}$	Definite integral over the entire domain of $\mathbf{x}$
$\int_{\mathbb{S}} f(\mathbf{x}) d\mathbf{x}$	Definite integral with respect to $\mathbf{x}$ over the set $\mathbb{S}$

### Probability and Information Theory

$P(a)$	A probability distribution over a discrete variable
$p(a)$	A probability distribution over a continuous variable, or over a variable whose type has not been specified
$a \sim P$	Random variable $a$ has distribution $P$
$\mathbb{E}_{x \sim P}[f(x)]$ or $\mathbb{E}f(x)$	Expectation of $f(x)$ with respect to $P(x)$
$\text{Var}(f(x))$	Variance of $f(x)$ under $P(x)$
$\text{Cov}(f(x), g(x))$	Covariance of $f(x)$ and $g(x)$ under $P(x)$
$H(x)$	Shannon entropy of the random variable $x$
$D_{\text{KL}}(P \  Q)$	Kullback-Leibler divergence of $P$ and $Q$
$\mathcal{N}(\mathbf{x}; \boldsymbol{\mu}, \boldsymbol{\Sigma})$	Gaussian distribution over $\mathbf{x}$ with mean $\boldsymbol{\mu}$ and covariance $\boldsymbol{\Sigma}$

### Functions

$f : \mathbb{A} \rightarrow \mathbb{B}$	The function $f$ with domain $\mathbb{A}$ and range $\mathbb{B}$
$f \circ g$	Composition of the functions $f$ and $g$
$f(\mathbf{x}; \boldsymbol{\theta})$	A function of $\mathbf{x}$ parametrized by $\boldsymbol{\theta}$ . (Sometimes we write $f(\mathbf{x})$ and omit the argument $\boldsymbol{\theta}$ to lighten notation)
$\log x$	Natural logarithm of $x$
$\sigma(x)$	Logistic sigmoid, $\frac{1}{1 + \exp(-x)}$
$\zeta(x)$	Softplus, $\log(1 + \exp(x))$
$\ \mathbf{x}\ _p$	$L^p$ norm of $\mathbf{x}$
$\ \mathbf{x}\ $	$L^2$ norm of $\mathbf{x}$
$x^+$	Positive part of $x$ , i.e., $\max(0, x)$
$\mathbf{1}_{\text{condition}}$	is 1 if the condition is true, 0 otherwise

---

## 6 FINAL INSTRUCTIONS

Do not change any aspects of the formatting parameters in the style files. In particular, do not modify the width or length of the rectangle the text should fit into, and do not change font sizes (except perhaps in the REFERENCES section; see below). Please note that pages should be numbered.

## 7 PREPARING POSTSCRIPT OR PDF FILES

Please prepare PostScript or PDF files with paper size “US Letter”, and not, for example, “A4”. The `-t letter` option on dvips will produce US Letter files.

Consider directly generating PDF files using pdflatex (especially if you are a MiKTeX user). PDF figures must be substituted for EPS figures, however.

Otherwise, please generate your PostScript and PDF files with the following commands:

```
dvips mypaper.dvi -t letter -Ppdf -G0 -o mypaper.ps  
ps2pdf mypaper.ps mypaper.pdf
```

### 7.1 MARGINS IN LATEX

Most of the margin problems come from figures positioned by hand using `\special` or other commands. We suggest using the command `\includegraphics` from the `graphicx` package. Always specify the figure width as a multiple of the line width as in the example below using `.eps` graphics

```
\usepackage[dvips]{graphicx} ...  
\includegraphics[width=0.8\linewidth]{myfile.eps}
```

or

```
\usepackage[pdftex]{graphicx} ...  
\includegraphics[width=0.8\linewidth]{myfile.pdf}
```

for `.pdf` graphics. See section 4.4 in the `graphics` bundle documentation (<http://www.ctan.org/tex-archive/macros/latex/required/graphics/grfguide.ps>)

A number of width problems arise when LaTeX cannot properly hyphenate a line. Please give LaTeX hyphenation hints using the `\- command`.

### AUTHOR CONTRIBUTIONS

If you’d like to, you may include a section for author contributions as is done in many journals. This is optional and at the discretion of the authors.

### ACKNOWLEDGMENTS

Use unnumbered third level headings for the acknowledgments. All acknowledgments, including those to funding agencies, go at the end of the paper.

## A APPENDIX

You may include other additional sections here.